Performance Analysis of a Second Order FLL Assisted Third Order PLL for Tracking Doppler Rates

MA Lu, SHI Liguo, WANG Zhugang
National Space Science Center
Chinese Academy of Sciences
Beijing, 100190
CHINA
iamroad@163.com

Abstract:-The comprehensive analysis of the Spread Spectrum Responder (SSR) carrier tracking loops is presented. A mathematical model of a second-order FLL assisted third-order PLL is illustrated to study the performance in dynamics and noise. A fixed point method is used in the work to analyze the stable regions for the FLL, PLL and FLL assisted PLL. The Chapman-Kolmogorov (C-K) equation is utilized to express the steady-state Probability Density Function (PDF) of these three loops. The steady-state mean and variance are also be derived. At last, we discuss the optimizations for the combined loop due to the fact that the assisted tracking loop can be considered as an equivalent third-order PLL. This work will play an important role in designing the high dynamic carrier tracking.

Key-Words: -Spread Spectrum; Fixed Point Problem; Frequency Locked Loop; Phase Locked Loop; FLL Assisted PLL; Probability Density Function

1 Introduction

The development of the aerospace measurement and control system (M&C) is based on the spacecraft's demand. The function and structure of telemetry, tracking and command (TT&C) for the spacecraft in the early days are simplex. M&C were realized by separated devices at different frequency channel. The Unified S-Band System (USB) was first introduced at 1960s. This system integrates various functions into one structure so as to get a simple and reliable one. But it is difficult to improve the range accuracy and track and control different objectives. Meanwhile, it has poor ability to resist interference. At 1970s, the Unified Spread Spectrum TT&C System was used to meet the demand of the complex space mission. Thegood anti-interference performance, high concealment and united code structure make the device easy to manage by realizing TT&C with one satellite [1,2].

Synchronization plays a key role in the receivers so as for the spread-spectrum responder (SSR): ±90kHz Doppler shift and 3kHz/s Doppler rates shall be compensated at the receiver side. This puts forward higher requirements for the carrier tracking structure due to the high dynamics. In this paper, we will study the tracking technique to meet the index [3].

This work is organized as follows. Section 2 presents the trajectory and DPLL model for SSR receiver, the analysis of the loop input signal, discriminator noise characteristics. The stable region, oscillatory behavior and steps to convergence of the second-order FLL, the third-order PLL and the FLL assisted PLL in the absence of noise are analyzed in Section 3. The mean and variance in the presence of noise for these three loops are discussed in Section 4. Section 5 studies the optimization of the assisted tracking loop followed by the conclusions in Section 6.

2System Modeling

Figure 1 shows the trajectory of the responder. At this point, we just consider the quadratic phase input as

$$\theta(t) = \theta_0 + 2\pi\left(f_0 t + \frac{f_1}{2} t^2 \right) + o(f) \qquad (1)$$

Where f_0 is Doppler shift and f1 is the Doppler rates. Although a great many literatures have discussed the methods to track Doppler rates such asKalman filter and the second-order PLL [4,5], we will study the second order FLL assisted thirdorder PLL due to the high dynamics and itssimplicity to implement on FPGA. The dynamic range, noise performance and loop optimization will be discussed in the paper.

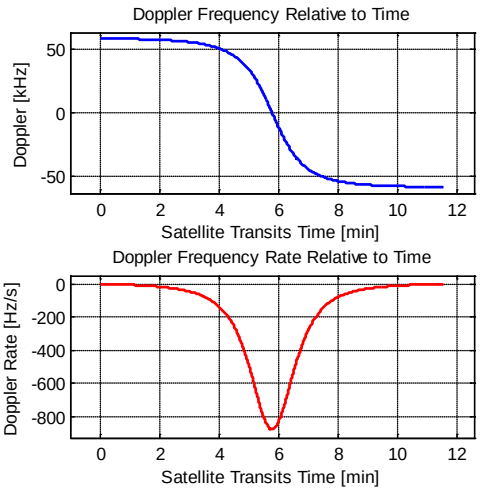

Fig 1. Trajectory of the spread-spectrum responder

2.1Loop Difference Equations

As shown in Figure 2, synchronization of PRN has achieved, we just focus on carrier synchronization. The NCO generates the local in-phase and quadrature reference signals at the sampling rate $f_s$for coherently correlating. The output of the loop filter modifies the phase and frequency of the NCO every NT_s. The m-*th* sample digital baseband processor (DBP) received signal at baseband is[6]

$$s[m]=\sqrt{2P}d[m]c[m]\times \sin\left(2\pi f_c m T_s+\theta[m]\right)+n[m] \quad (2)$$

Where, P is the signal power, d[m] represents the baseband signal, c[m] is spread code, $f_c(1/T_s)$ represents the sample frequency.

The in-phase and in-quadrature correlation of the received signal with the locally generated replicas are inputs to the tracking loops. They can be expressed for the *k-th* integration interval as

$$\begin{aligned} I_k &= A_k\cos(\varphi_k)+n_i[k] \\ Q_k &= A_k\sin(\varphi_k)+n_q[k] \end{aligned} \quad (3)$$

Where, $A_k=\sqrt{P}d_k R(\tau_k)\sin c(\delta\omega_k T_L/2)$ is the results of correlation, $\varphi_k=\delta\theta_k=\theta_k-\hat{\theta}_k$ is the phase estimation error, τ_k、$\delta\theta_k$ and $\delta\omega_k$ are the averaged code phase, carrier phase estimation error and radian frequency estimation error. T_L is the integrations time, R(·) is the code correlation function, and sinc(*x*)=sin(π*x*)/(π*x*). This expression assumes that the data bit d[m] and the received signal radian frequency ω_k remain constant during the integration time.

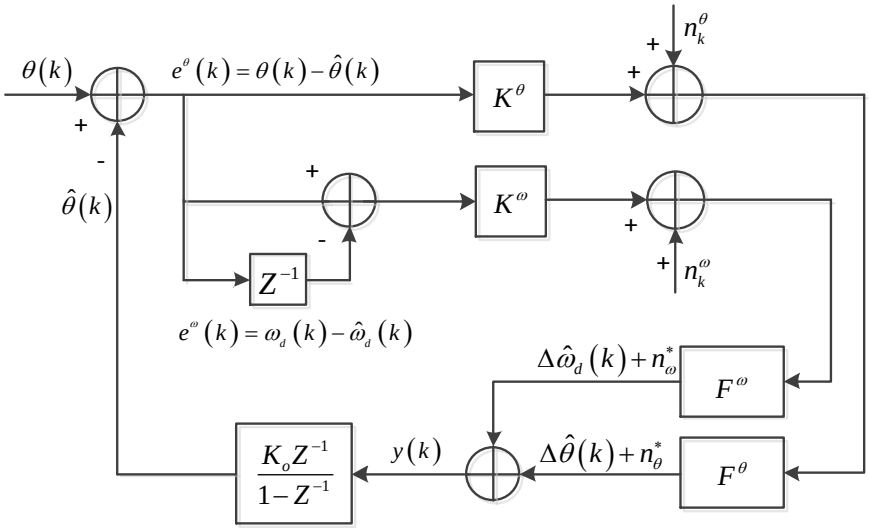

Fig. 2. Structure of a second order FLL assisted third PLL

Frequency error can be got by taking derivation of the two successive phases as[7]

$$\begin{aligned} Dot(k) &= I(k-1)I(k)+Q(k-1)Q(k) \\ Cross(k) &= I(k-1)Q(k)-I(k)Q(k-1) \end{aligned} \quad (4)$$

The linear frequency discriminator and phase discriminator perform an four quadrant arctangent and an two quadrant arctangent, which have outputs as [8]

$$\begin{aligned} e^{\omega}(k) &= \arctan 2\left[\frac{Dot(k)}{Cross(k)}\right]=\frac{g^{\omega}[w_k]}{T_L}+n_k^{\omega} \\ e^{\omega}(k) &\in \frac{[-\pi,+\pi]}{T_L},\quad w_k=\varphi_k-\varphi_{k-1} \end{aligned} \quad (5)$$

$$\begin{aligned} e^{\theta}(k) &= \arctan\left[Q(k)/I(k)\right]=g^{\theta}[\varphi_k]+n_k^{\theta} \\ e^{\theta}(k) &\in [-\pi/2,+\pi/2] \end{aligned} \quad (6)$$

Where $g^{\theta}[\cdot]$ and $g^{\omega}[\cdot]$are the characteristic functions of the frequency discriminator and phase discriminator, respectively. While φ(k) is the phase tracking error due to a noise-free incoming signal and $n^{\theta}(k) \in (-\pi/2-g^{\theta}[\varphi(k)], +\pi/2-g^{\theta}[\varphi(k)])$ is the phase disturbance due to the input noise; w(k) is the phase tracking error due to a noise-free incoming signal and $n^{\omega}(k) \in (-\pi-g^{\omega}[\varphi(k)], +\pi-g^{\omega}[\varphi(k)])/T_L$ is the phase disturbance due to the input noise.Due to the linear characteristic of arctangent discriminators, the characteristic functions of this two discriminators are

$$\begin{aligned} g^{\theta}[w_k] &= w_k \bmod [-\pi, +\pi] \\ g^{\omega}[\varphi_k] &= \varphi_k \bmod [-\pi/2, +\pi/2] \end{aligned} \tag{7}$$

A mathematically equivalent model of the FLL assisted PLL is show in Fig. 1. With the NCO transfer function $N(z)=z^{-1}/(1-z^{-1})$ and loop filter $F^{\theta}(z)$ and $F^{\omega}(z)$, the corresponding loop equations are

$$\begin{aligned} &\varphi(k) = \theta(k) - \hat{\theta}(k) \\ &e^{\theta}(k) = g^{\theta}[\varphi(k)] + n^{\theta}(k) \\ &e^{\omega}(k) = g^{\omega}[\varphi(k)] + n^{\omega}(k) \\ &y(k) = F^{\theta}(z)e^{\theta}(k) + D(z)F^{\omega}(z)e^{\omega}(k) \\ &\hat{\theta}(k) = N(z)y(k) = \sum_{i=0}^{k-1} y(i) \end{aligned} \tag{8}$$

The expressions for D(z), N(z), $F^{\omega}(z)$ and $F^{\theta}(z)$ are

$$D(z) = 1 - z^{-1} \tag{9}$$

$$N(z) = \frac{K_o z^{-1}}{1 - z^{-1}} \tag{10}$$

$$F^{\omega}(z) = \left(C_1^{\omega} + \frac{C_2^{\omega}}{1 - z^{-1}} \right) \cdot \frac{1}{1 - z^{-1}} \tag{11}$$

$$F^{\theta}(z) = C_1^{\theta} + \frac{C_2^{\theta}}{1 - z^{-1}} + \frac{C_3^{\theta}}{\left(1 - z^{-1}\right)^2} \tag{12}$$

The filters' structure of the second frequency locked loop (FLL) assisted the third order phase locked loop[7] (PLL) is illustrated in Figure 3.

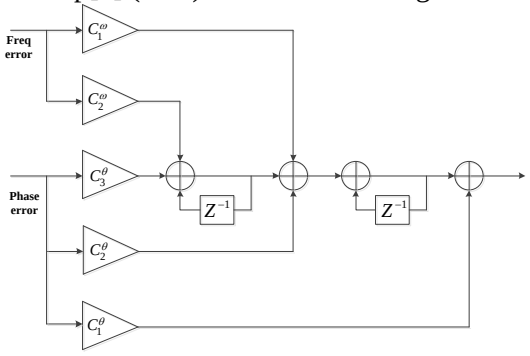

Fig3. Filters' structure of second order FLL assisted third order PLL

2.2Characteristics of Discriminator Noise

The discussion below focuses on the noise distribution of phase discriminator, the calculation method also suits frequency discriminator by replacing the $\varphi_k$of eq. (19) with the frequency error w_k.

The signal envelope and phase estimation error is obtain by

$$Z_k = \sqrt{I_k^2 + Q_k^2}, \quad Z_k \geq 0 \tag{13}$$

$$e_k = \arctan\left(\frac{Q_k}{I_k}\right), \quad -\pi \leq e_k \leq \pi \tag{14}$$

It has been shown that n_i and n_q in (2) are Gaussian if $N \geq 1$, and the means and variances of I_k and Q_k can be expressed as follows [6]

$$\begin{aligned} &E[I_k] = A_k \cos(\varphi_k), \quad E[Q_k] = A_k \sin(\varphi_k) \\ &Var(I_k) = Var(Q_k) = \frac{N_0}{2T_L} = \sigma_k^2 \end{aligned} \tag{15}$$

Where, $Var(x)$ represents the variance of x.

Given the phase estimation error φ_k, the joint probability density function (PDF) between I_k and Q_k is

$$\begin{aligned} p(I_k, Q_k/\varphi_k) = \frac{1}{2\pi\sigma_k^2} \exp\left\{ -\frac{1}{2\sigma_k^2} \left[\left(I_k - A_k \cos(\varphi_k)\right)^2 \right.\right. \\ \left.\left. + \left(Q_k - A_k \sin(\varphi_k)\right)^2 \right] \right\} \end{aligned} \tag{16}$$

According to the following relationship between I_k, Q_k and Z_k, φ_k

$$\begin{cases} I_k = Z_k \cos(e_k) \\ Q_k = Z_k \sin(e_k) \end{cases} \tag{17}$$

The joint PDF of the envelope Z_k and phase estimation error φ_k can be calculated by

$$p(Z_k, e_k/\varphi_k) = p(I_k, Q_k/\varphi_k) \cdot \left| \frac{\partial(I_k, Q_k)}{\partial(Z_k, e_k)} \right| =$$

$$\begin{aligned} Z_k \cdot p(I_k, Q_k/\varphi_k) = \frac{Z_k}{2\pi\sigma_k^2} \exp\left\{ -\frac{1}{2\sigma_k^2} \times \right. \\ \left. \left[Z_k^2 + A_k^2 - 2Z_k A_k \cos(\varphi_k - e_k) \right] \right. \end{aligned} \tag{18}$$

Integrating (18) with respect to Z_k from 0 to ∞, we obtain the conditional probability density function(CPDF) of phase error[9,10].

$$p(e_k/\varphi_k)=\frac{1}{2\pi}\exp(-SNR)+\frac{1}{2}\sqrt{\frac{SNR}{\pi}}\cos(\varphi_k-e_k)\times\exp\left\{-SNR\cdot\sin^2(\varphi_k-e_k)\right\}\times\left[1+erf\left(\sqrt{SNR}\cos(\varphi_k-e_k)\right)\right] \quad (19)$$

where $erf(x)=2/\sqrt{\pi}\cdot\int_0^x e^{-u^2}du$ is the Gaussian error function, $SNR=A_k^2/2\sigma_k^2$ is the signal to noise ratio (SNR) after correlation. Figure 4 depicts the CPDF at six different SNRs in the form of eq.(19).

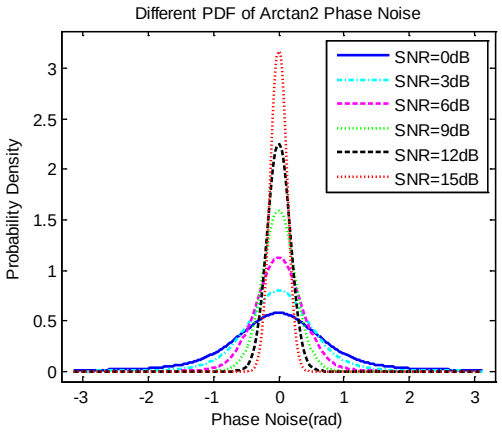

Fig 4. PDF of Discriminator Noise at Different SNRs

According to (6), we have the PDF of the discriminator noise as

$$p(n_k)=\frac{1}{2\pi}\exp(-SNR)+\frac{1}{2}\sqrt{\frac{SNR}{\pi}}\cos(n_k)\times\exp\left\{-SNR\cdot\sin^2(n_k)\right\}\times\left[1+erf\left(\sqrt{SNR}\cos(n_k)\right)\right] \quad (20)$$

where n_k is n_k^{ω} or n_k^{θ} depends on the discriminate parameter, that is frequency or phase.

From the above discussion, the output of the discriminators consist of both error $g_1[\varphi_k]$ or $g_2[w_k]$ due to incoming signal phase dynamics and error $n^{\theta}(k)$ or $n^{\omega}(k)$ due to incoming additive noise. In the following, we analyze the error component resulting from system dynamics in Section 3 and from noise in Section 4.

3DYNAMIC PERFORMANCE IN THE ABSENCE OF NOISE

In this section, we will analyze the linearity of the loop by studying the equation as a fixed-point problem. This makes available contractive mapping theorems which determine convergence to a steady-state solution and gives results which are rigorously correct. What's more, by using this theorems, we can obtain bounds on the rate of convergence (acquisition time) to the fixed point (steady-state solution) for a frequency ramp input.

We will first analyze the dynamic performance of the second-order FLL, because the stability of the FLL determines the overall stabilization of the combined tracking loops; then the third order PLL dynamics will be studied. At last, we will present the stable region of the assisted tracking loops.

3.1 The Second-Order FLL

In the absence of input noise, the random frequency noise $n^{\omega}(k)$ vanish so that $e_{\omega}(k)=g_1[w(k)]$ mod $[-\pi,+\pi]$. The frequency transfer function can be expressed in terms of the loop filter $F^{\omega}(z)$, the numerically controlled oscillator N(z) and the discriminator function D(z) as[6]

$$H^{\omega}(z)=\frac{\hat{\Omega}(z)}{\Omega(z)}=\frac{K^{\omega}D(z)F^{\omega}(z)N(z)}{1+K^{\omega}D(z)F^{\omega}(z)N(z)} \quad (21)$$

Also, we have

$$\Phi(z)=\frac{\Theta(z)}{1+K^{\omega}D(z)F^{\omega}(z)N(z)} \quad (22)$$

where $D(z)=1-Z^{-1}$, it's the phase difference function.$\Theta(z)$ and $\Phi(z)$ are the z transformations of $\theta(k)$ and $\varphi(k)$.

The loop locking condition and frequency tracking error in the absence of noise will be analyzed based on (22).The loop difference equation of the second order FLL is

$$\varphi(k)-2\varphi(k-1)+\varphi(k-2)=[\theta(k)-2\theta(k-1)+\theta(k-2)]-\left(G_1^{\omega}+G_2^{\omega}\right)\varphi(k-1)+G_1^{\omega}\varphi(k-2) \quad (23)$$

where $G_1^{\omega}=K_oK^{\omega}C_1^{\omega}, G_2^{\omega}=K_oK^{\omega}C_2^{\omega}$.

Equation (21) defines the linear difference equation of loop operation for FLL. In studying the dynamical response of the loop to the Doppler rates inputs, we shall be concerned with the conditions under which the above equation exhibits a steady-state response since this indicates whether the loop will lock. This problem can be stated as a fixed point problem. The loop equation is of the form[11,12]

$$x_{m+1}=G(x_m) \quad (24)$$

And what we are seeking is a solution x^* such that

$$x^*=G(x^*) \quad (25)$$

If (25) is satisfied, then x^* is called a fixed point of G, and under certain conditions, the sequence $\{x_i\}$

defined by (24) will converge to the solution x^*.
We assume the input is a quadratic phase input, i.e.,

$$\theta_k = \theta + \omega \cdot t_k + \frac{1}{2}\Omega_1 \cdot t_k^2 \triangleq a_0 + a_1 k + a_2 k^2 \quad (26)$$

Substitute (26) into (23) yields

$$\begin{aligned} &\varphi(k) - 2\varphi(k-1) + \varphi(k-2) \\ &\quad = 2a_2 - \left(G_1^{\omega} + G_2^{\omega}\right)\varphi(k-1) + G_1^{\omega}\varphi(k-2) \end{aligned} \quad (27)$$

Also we can expressed as

$$\varphi_{k+2} - 2\varphi_{k+1} + \varphi_k = 2a_2 - \left(G_1^{\omega} + G_2^{\omega}\right)\varphi_{k+1} + G_1^{\omega}\varphi_k \quad (28)$$

It is easy to see that the fixed point is

$$\varphi^* = \frac{2a_2}{G_2^{\omega}} \quad (29)$$

3.1. 1 Range of Gain for Stability

In order to apply the fixed point method, we must transform the equation into a system of two first-order equations, so it is in the form $x_{k+1}=G(x_k)$. Thus, if $y_k=\varphi_{k+1}$, $x_k=\varphi_k$, then equation (28) becomes

$$\begin{aligned} \begin{bmatrix} x_{k+1} \\ y_{k+1} \end{bmatrix} &= \begin{bmatrix} y_k \\ 2a_2 + \left(2 - r^{\omega}G_1^{\omega}\right)y_k + \left(G_1^{\omega} - 1\right)x_k \end{bmatrix} \\ &\triangleq \begin{bmatrix} g_1(x_k) \\ g_2(x_k) \end{bmatrix} \triangleq G(\vec{x}_k) \end{aligned} \quad (30)$$

where, $x_k=\varphi_k$, $x_0=(\varphi_0, \varphi_1)^T$.and

$$r^{\omega} = 1 + \frac{G_2^{\omega}}{G_1^{\omega}} \quad (31)$$

The Jacobian $G'(x)=(\partial g_i/\partial x^j)$ is given by

$$G'(x) = \begin{bmatrix} 0 & 1 \\ G_1^{\omega} - 1 & 2 - r^{\omega}G_1^{\omega} \end{bmatrix} \quad (32)$$

In order to have the eigenvalues of $G'(x)$ less than 1, we must have

$$0 < G_1^{\omega} < \frac{4}{1 + r^{\omega}}, \quad r^{\omega} > 1 \quad (33)$$

The conditions for faster convergence, i.e., $\rho[G'(x^*)] = 0$, can be obtained by examining (32); these are

$$G_1^{\omega} = 1, \quad r^{\omega}G_1^{\omega} = 2 \quad (34)$$

Then the matrix has three zero elements and its spectral radius is zero. Since the rate of convergence near the fixed point can be show to be governed by the spectral radius, we shall take $G_1^{\omega}=1$ and $rG_1^{\omega}=2$ as our "optimum" values in terms of acquisition time.

It is to be noted that since the convergence condition (33) has been obtain assuming that φ(k)'s lie between –π and π, the condition guarantees locking only in the neighborhood of the steady-state error in which φ(k) does not cause φ(k+1) to be outside the interval (-π, π). Thus, for φ(k) to converge to the fixed point, independently of the initial phase error, another condition $|\varphi(k+1)|<\pi$ for all k is required. This condition leads to the following four expressions[8].

a. when $\varphi(k)=\pi$ and $\varphi(k+1)=\pi$, we have $|\varphi(k+2)|<\pi$, thus

$$\frac{2a_2}{\pi} < \left(r^{\omega} - 1\right)G_1^{\omega} < 2 + \frac{2a_2}{\pi}$$

b. when $\varphi(k)=\pi$ and $\varphi(k+1)=-\pi$, we have $|\varphi(k+2)|<\pi$, thus

$$2 - \frac{2a_2}{\pi} < \left(r^{\omega} + 1\right)G_1^{\omega} < 4 - \frac{2a_2}{\pi}$$

c. when $\varphi(k)=-\pi$ and $\varphi(k+1)=\pi$, we have $|\varphi(k+2)|<\pi$, thus

$$2 + \frac{2a_2}{\pi} < \left(r^{\omega} + 1\right)G_1^{\omega} < 4 + \frac{2a_2}{\pi}$$

d. when $\varphi(k)=\pi$ and $\varphi(k+1)=\pi$, we have $|\varphi(k+2)|<\pi$, thus

$$-\frac{2a_2}{\pi} < \left(r^{\omega} - 1\right)G_1^{\omega} < 2 - \frac{2a_2}{\pi}$$

From the above analysis, convergence conditions which are independent of the initial phase errors can be concluded as

$$\begin{aligned} \frac{2|a_2|}{\pi} &< \left(r^{\omega} - 1\right)G_1^{\omega} < 2 - \frac{2|a_2|}{\pi} \\ 2 + \frac{2|a_2|}{\pi} &< \left(r^{\omega} + 1\right)G_1^{\omega} < 4 - \frac{2|a_2|}{\pi} \end{aligned} \quad (35)$$

The stable regions for the loop parameters are plotted on G_1^{ω}-r plane in Fig. 5 with dynamic parameter: $a_2=\pi/4$. The transient responses are plotted in Fig. 6 for $G_1^{\omega}=1$ and r=1.5, 2 and 2.5 with initial phase errors $\varphi(0)=0$ and $\varphi(1)=1$, given the input phase $\theta(k)=0.125k^2+0.5k+1$. It is observed that the steady-state phase tracking error reduces with the increase of loop parameter *r* and the fast convergence is achieved at *r*=2. This is in accordance with equation (34).

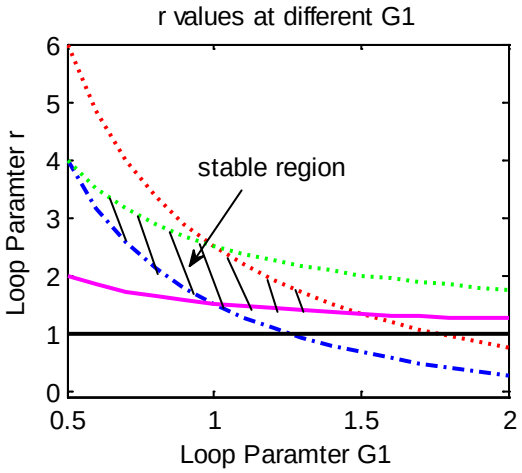

Fig. 5. The second order FLL stable region

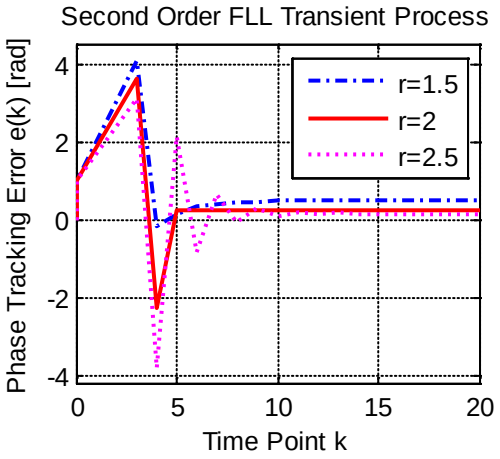

Fig. 6. The second order FLL transient response

3.1.2Number of Steps for Convergence

In order to calculate the steps for convergence, we need first extend the theory in [12] to higher dimensions as:

Theorem 1[12]: Suppose that X is a normed vector space and K is a subset of X such that the following conditions hold:

1) G: K→K
2) $G(x^*)=x^*$, $x^* \in K$
3) There exists a constant L: $0 \le L < 1$ such that

$$\left\| G(\vec{x}) - G(\vec{x}^*) \right\| \le L \left\| \vec{x} - \vec{x}^* \right\|, \quad \forall x \in K$$

Then the following conclusions can be made:

1) $\lim_{m\to\infty} \vec{x}_m = \vec{x}^*, \quad \forall \vec{x}_0 \in K$

and x^* is the unique fixed point of G in K.

2) $\left\| \vec{x}_m - \vec{x}^* \right\| \le L^m \left\| \vec{x}_0 - \vec{x}^* \right\|$

Based on this theory, the steps for convergence to a radius ε beside the stationary point can be represented as[11,12]

$$m < \frac{\ln\left(\dfrac{\varepsilon}{\left[(\varphi_0 - \varphi_{ss})^2 + (\varphi_1 - \varphi_{ss})^2 \right]} \right)}{\ln(L)} \quad (36)$$

Where φ_0 and φ_1 are the initial phase errors, φ_{ss} is the stationary phase error, arguments ψ_0 and ψ_1 satisfy $\psi_0 \in [-\varphi_0, \varphi_0]$, $\psi_1 \in [-\varphi_1, \varphi_1]$and L satisfies the following equation

$$L = \max \left\{ \begin{array}{l} \dfrac{\left[\left(2 - r^{\omega} G_1^{\omega}\right)\psi_1 + \left(G_1^{\omega} - 1\right)\psi_0 + 2a_2 - \varphi_{ss} \right]^2}{\left[(\varphi_0 - \varphi_{ss})^2 + (\varphi_1 - \varphi_{ss})^2 \right]} \\ + \dfrac{(\psi_0 - \varphi_{ss})^2}{\left[(\varphi_0 - \varphi_{ss})^2 + (\varphi_1 - \varphi_{ss})^2 \right]} \end{array} \right\} \quad (37)$$

3.1.3 Oscillatory Behavior

We now examine the behavior of the phase error for loop parameters outside the bounds given in (3.1.13). An oscillatory solution exits[11,12] where

$$\begin{aligned} \varphi_2 &= 2a_2 + \left(2 - r^{\omega} G_1^{\omega}\right)\varphi_1 + \left(G_1^{\omega} - 1\right)\varphi_2 \\ \varphi_1 &= 2a_2 + \left(2 - r^{\omega} G_1^{\omega}\right)\varphi_2 + \left(G_1^{\omega} - 1\right)\varphi_1 \end{aligned} \quad (38)$$

These yields

$$\varphi_1 = \varphi_2 = \frac{2a_2}{G_2^{\omega}}$$

It is easy to see that these two oscillatory points are the same as the steady-state point and this situation also suits for the three oscillatory points. This result illustrates that if the loop oscillates at some particular points then these points are the same to the only one stationary point and loop operates on the stable regions. Otherwise, the loop will oscillate with increasing amplitude like Fig. 7.

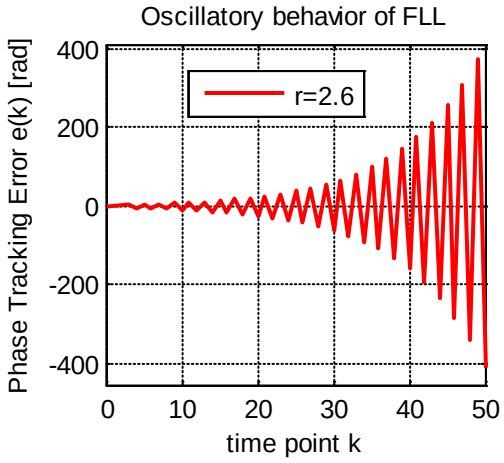

Fig. 7. Oscillatory Behavior of the second order FLL

3.2 The Third-Order PLL

As for the third order PLL, the loop transfer function is[6]

$$\Phi(z)=\frac{\Theta(z)}{1+K^{\theta}F^{\theta}(z)N(z)} \tag{39}$$

By expending the function we have

$$\begin{aligned}&\Theta(z)\left(1-3z^{-1}+3z^{-2}-z^{-3}\right)\\&=\Phi(z)\left[1+\left(G_1^{\theta}+G_2^{\theta}+G_3^{\theta}-3\right)z^{-1}\right.\\&\left.-\left(2G_1^{\theta}+G_2^{\theta}-3\right)z^{-2}+\left(G_1^{\theta}-1\right)z^{-3}\right]\end{aligned} \tag{40}$$

The corresponding difference equation is

$$\begin{aligned}&\theta_k-3\theta_{k-1}+3\theta_{k-2}-\theta_{k-3}\\&=\varphi_k+\left(p^{\theta}G_1^{\theta}-3\right)\varphi_{k-1}-\left[\left(1+r^{\theta}\right)G_1^{\theta}-3\right]\varphi_{k-2}\\&+\left(G_1^{\theta}-1\right)\varphi_{k-3}\end{aligned} \tag{41}$$

Here, the loop parameters are

$$p^{\theta}=1+\frac{G_2^{\theta}}{G_1^{\theta}}+\frac{G_3^{\theta}}{G_1^{\theta}},\quad r^{\theta}=1+\frac{G_2^{\theta}}{G_1^{\theta}} \tag{42}$$

For a quadratic phase input, the difference equation can be expressed as

$$\begin{aligned}&\varphi_{k+3}+\left(p^{\theta}G_1^{\theta}-3\right)\varphi_{k+2}\\&-\left[\left(1+r^{\theta}\right)G_1^{\theta}-3\right]\varphi_{k+1}+\left(G_1^{\theta}-1\right)\varphi_k=0\end{aligned} \tag{43}$$

It is easy to see that the stationary solution of (43) is

$$\varphi^{*}=0 \tag{44}$$

3.2.1 Range of Gain for Stability

The equation (43) can be expressed as a system of three first-order equations, so it is in the form $x_{k+1}=G(x_k)$.

Thus, if $z_k=\varphi_{k+2}$, $y_k=\varphi_{k+1}$, $x_k=\varphi_k$, then equation (43) becomes

$$\begin{bmatrix}x_{k+1}\\y_{k+1}\\z_{k+1}\end{bmatrix}=\begin{bmatrix}y_k\\z_k\\-\left(p^{\theta}G_1^{\theta}-3\right)z_k\\\quad+\left[\left(1+r^{\theta}\right)G_1^{\theta}-3\right]y_k-\left(G_1^{\theta}-1\right)x_k\end{bmatrix} \tag{45}$$

where, $x_k=\varphi_k$, $x_0=(\varphi_0, \varphi_1, \varphi_2)^{T}$.

The Jacobian $G'(x)=(\partial g_i/\partial x^j)$ is given by

$$G'(x)=\begin{bmatrix}0 & 1 & 0\\0 & 0 & 1\\1-G_1^{\theta} & \left(1+r^{\theta}\right)G_1^{\theta}-3 & 3-p^{\theta}G_1^{\theta}\end{bmatrix} \tag{46}$$

At the fixed point $x^{*}=0$, we must have $|\lambda_i|<1$, i=1, 2, 3. where the λ's satisfy the characteristic equation $|\lambda I- G'(x^{*})|= 0$ or

$$\lambda^3+\lambda^2\left(p^{\theta}G_1^{\theta}-3\right)+\lambda\left[3-\left(1+r^{\theta}\right)G_1^{\theta}\right]+G_1^{\theta}-1=0 \tag{47}$$

The Routh-Hurwitz criteria can be used to obtain stability bounds for (46) if the following transformation is used to map the interior of the unit circle to the left half-plan[12]:

$$\lambda=\frac{v+1}{v-1} \tag{48}$$

Substitute this transformation into (47), the resulting equation in v is

$$\begin{aligned}&v^3\left(p^{\theta}G_1^{\theta}-r^{\theta}G_1^{\theta}\right)+v^2\left(p^{\theta}G_1^{\theta}+r^{\theta}G_1^{\theta}-G_1^{\theta}\right)\\&+v\left(-p^{\theta}G_1^{\theta}+r^{\theta}G_1^{\theta}+4G_1^{\theta}\right)\\&+\left(8-p^{\theta}G_1^{\theta}-r^{\theta}G_1^{\theta}-2G_1^{\theta}\right)=0\end{aligned} \tag{49}$$

When applying the Routh-Hurwitz criteria[11,12], we have the stable conditions for the coefficients

$$\begin{aligned}&p^{\theta}-r^{\theta}>0\\&p^{\theta}+r^{\theta}-2>0\\&4-p^{\theta}+r^{\theta}>0\\&8-G_1^{\theta}\left(p^{\theta}+r^{\theta}+2\right)>0\\&G_1^{\theta}\left(p^{\theta}-1\right)-p^{\theta}+r^{\theta}>0\end{aligned} \tag{50}$$

The faster convergence can be achieved when applying $\rho[G'(x^{*})] = 0$ by examining (46); these are

$$G_1^{\theta}=1,\quad r^{\theta}=2,\quad p^{\theta}=3 \tag{51}$$

It is also required that $|\varphi_{k+3}|<\pi$ when $|\varphi_{k+2}|=\pi$, $|\varphi_{k+1}|=\pi$, $|\varphi_k|=\pi$ [8]. So the overall loop stable conditions independent of the initial phase tracking error can be further derived asthe following expressions.

a. when $\varphi(k+2)=\pi$, $\varphi(k+1)=\pi$ and $\varphi(k)=\pi$, we have $|\varphi(k+3)|<\pi$, thus

$$-2<\left(r^{\theta}-p^{\theta}\right)G_1^{\theta}<0$$

b. when $\varphi(k+2)=\pi$, $\varphi(k+1)=\pi$ and $\varphi(k)=-\pi$, we have $|\varphi(k+3)|<\pi$, thus

$$0<\left(2+r^{\theta}-p^{\theta}\right)G_1^{\theta}<2$$

c. when $\varphi(k+2)=\pi$, $\varphi(k+1)=-\pi$ and $\varphi(k)=\pi$, we have $|\varphi(k+3)|<\pi$, thus

$$6<\left(p^{\theta}+r^{\theta}+2\right)G_1^{\theta}<8$$

d. when $\varphi(k+2)=\pi$, $\varphi(k+1)=-\pi$ and $\varphi(k)=-\pi$, we have $|\varphi(k+3)|<\pi$, thus

$$4<\left(p^{\theta}+r^{\theta}\right)G_1^{\theta}<6$$

e. when $\varphi(k+2)=-\pi$, $\varphi(k+1)=\pi$ and $\varphi(k)=\pi$, we have $|\varphi(k+3)|<\pi$, thus

$$4 < \left(p^{\theta} + r^{\theta}\right) G_1^{\theta} < 6$$

f. when φ(*k*+2)=-π, φ(*k*+1)=π and φ(*k*)=-π, we have |φ(*k*+3)|<π, thus

$$6 < \left(p^{\theta} + r^{\theta} + 2\right) G_1^{\theta} < 8$$

g. when φ(*k*+2)=-π, φ(*k*+1)=-π and φ(*k*)=π, we have |φ(*k*+3)|<π, thus

$$0 < \left(2 + r^{\theta} - p^{\theta}\right) G_1^{\theta} < 2$$

h. when φ(*k*+2)=-π, φ(*k*+1)=-π and φ(*k*)=-π, we have |φ(*k*+3)|<π, thus

$$-2 < \left(r^{\theta} - p^{\theta}\right) G_1^{\theta} < 0$$

The above analysis can be concluded as

$$\begin{aligned} -2 &< \left(r^{\theta} - p^{\theta}\right) G_1^{\theta} < 0 \\ 0 &< \left(2 + r^{\theta} - p^{\theta}\right) G_1^{\theta} < 2 \\ 6 &< \left(p^{\theta} + r^{\theta} + 2\right) G_1^{\theta} < 8 \\ 4 &< \left(p^{\theta} + r^{\theta}\right) G_1^{\theta} < 6 \end{aligned} \tag{52}$$

According to (52), the stable region on the *r*-*p* plane of loop parameters is show in Fig. 8 with G_1^{θ}=1. The stable regions are invariant when just consider the quadratic phase input. Figs. 9 and 10 shows the loop transient responses with initial phase error φ(-2)= φ(-1)=0, φ(0)=1(rad) and G_1^{θ}=1, r^{θ}=1.5, 2 ,3 and p^{θ}=2.5, 3 ,3.5. It is noticed that whatever the loop gain parameters change while inside the stable regions, the loop will converge to zero steady-state phase error, and the fast convergence is achieved with G_1^{θ}=1, r^{θ}=2 and p^{θ}=3.

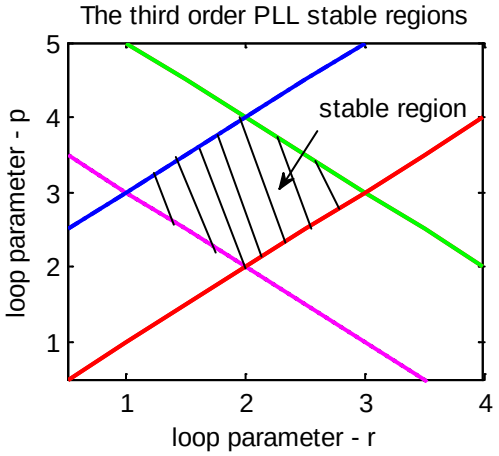

Fig. 8The third order PLL stable regions

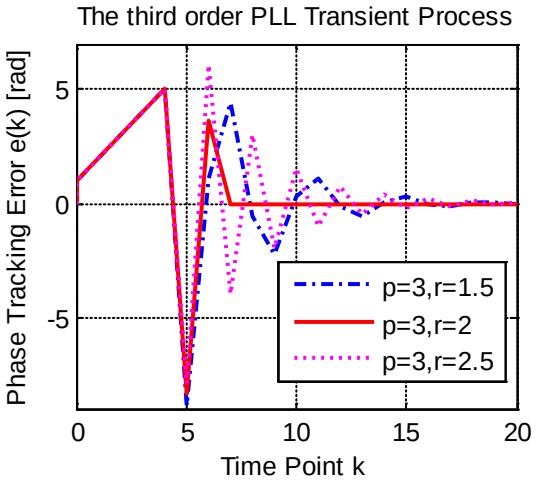

Fig. 9 FLL assisted PLL transient processes; G_1=1.0, φ(-2)= φ(-1)=0, φ(0)=1(rad) *p*=3 and *r*=1.5, 2, 2.5

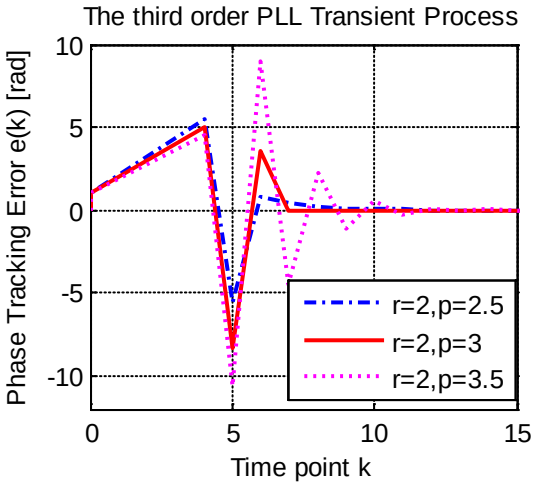

Fig. 10 FLL assisted PLL transient processes; G_1=1.0, φ(-2)= φ(-1)=0, φ(0)=1(rad) *r*=2 and *p*=2.5, 3, 3.5

3.2.2 Number of Steps for Convergence

Applying the method of Section 3.1.2, the steps to convergences is

$$m < \frac{\ln\left(\dfrac{\varepsilon}{\sqrt{\left[\left(\varphi_0 - \varphi_{ss}\right)^2 + \left(\varphi_1 - \varphi_{ss}\right)^2 + \left(\varphi_2 - \varphi_{ss}\right)^2\right]}}\right)}{\ln\left(L\right)} \tag{53}$$

And L satisfies

$$L=\max\left\{\begin{array}{l}\dfrac{\left[\left(3-p^{\theta}G_1^{\theta}\right)\psi_2+\left(\left(1+r^{\theta}\right)G_1^{\theta}-3\right)\psi_1-\left(G_1^{\theta}-1\right)\psi_0-\varphi_{ss}\right]^2}{\left[\left(\varphi_0-\varphi_{ss}\right)^2+\left(\varphi_1-\varphi_{ss}\right)^2+\left(\varphi_2-\varphi_{ss}\right)^2\right]}\\ +\dfrac{\left(\psi_1-\varphi_{ss}\right)^2}{\left[\left(\varphi_0-\varphi_{ss}\right)^2+\left(\varphi_1-\varphi_{ss}\right)^2+\left(\varphi_2-\varphi_{ss}\right)^2\right]}\\ +\dfrac{\left(\psi_0-\varphi_{ss}\right)^2}{\left[\left(\varphi_0-\varphi_{ss}\right)^2+\left(\varphi_1-\varphi_{ss}\right)^2+\left(\varphi_2-\varphi_{ss}\right)^2\right]}\end{array}\right\}$$

Where φ_0, $\varphi_1$and$\varphi_2$are the initial phase errors, φ_{ss} is the stationary phase error, arguments ψ_0, $\psi_1$and$\psi_2$satisfy $\psi_0\in[-\varphi_0, \varphi_0]$, $\psi_1\in[-\varphi_1, \varphi_1]$, $\psi_2\in[-\varphi_2, \varphi_2]$.

3.2.3 Oscillatory Behavior

We now examine the behavior of the phase error for loop parameters outside the bounds given in (50). An oscillatory solution exits where

$$\begin{aligned}\varphi_2&=\left(p^{\theta}G_1^{\theta}-3\right)\varphi_1-\left[\left(1+r^{\theta}\right)G_1^{\theta}-3\right]\varphi_2+\left(G_1^{\theta}-1\right)\varphi_1\\ \varphi_1&=\left(p^{\theta}G_1^{\theta}-3\right)\varphi_2-\left[\left(1+r^{\theta}\right)G_1^{\theta}-3\right]\varphi_1+\left(G_1^{\theta}-1\right)\varphi_2\end{aligned}\quad(54)$$

These yields

$$\varphi_1=\varphi_2=0$$

These two oscillatory points are the same as the steady-state point and this situation also suits for three or four oscillatory points. This situation is similar to that of the second FLL. The stable oscillatory point is unique and equals to zero. The other oscillatory situations occur at unstable regions as Fig. 11.

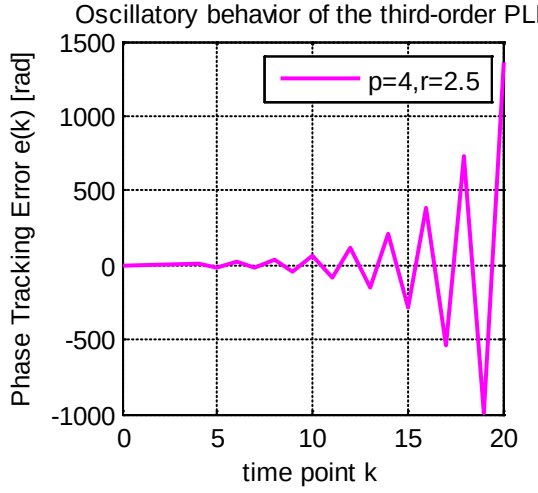

Fig. 11. Oscillatory Behavior of the third order PLL

3.3 The Combined Tracking Loop

In the assisted carrier phase fine tracking, loop can be represented on z-plane as[6,8]

$$\Phi(z)=\frac{\Theta(z)}{1+\left[K^{\theta}F^{\theta}(z)+D(z)K^{\omega}F^{\omega}(z)\right]N(z)}\quad(55)$$

Substitute (9)、(10)、(11) and (12) into (55), therefore, the combined tracking loop equation is

$$\begin{aligned}&\Theta(z)\left(1-3z^{-1}+3z^{-2}-z^{-3}\right)\\&=\Phi(z)\left[1+\left(G_1^{\theta}+G_2^{\theta}+G_3^{\theta}+G_1^{\omega}+G_2^{\omega}-3\right)z^{-1}\right.\\&\quad-\left(2G_1^{\theta}+G_2^{\theta}+2G_1^{\omega}+G_2^{\omega}-3\right)z^{-2}\\&\quad\left.+\left(G_1^{\theta}+G_1^{\omega}-1\right)z^{-3}\right]\end{aligned}\quad(56)$$

Where, the coefficients of the filter are

$$\begin{aligned}&G_1^{\theta}=K_oK^{\theta}C_1^{\theta},G_2^{\theta}=K_oK^{\theta}C_2^{\theta}\\&G_3^{\theta}=K_oK^{\theta}C_3^{\theta},G_1^{\omega}=K_oK^{\omega}C_1^{\omega}\\&G_2^{\omega}=K_oK^{\omega}C_2^{\omega}\end{aligned}\quad(57)$$

The difference equation characterizing loop performance becomes

$$\begin{aligned}&\theta_k-3\theta_{k-1}+3\theta_{k-2}-\theta_{k-3}\\&=\varphi_k+K_1\varphi_{k-1}-K_2\varphi_{k-2}+K_3\varphi_{k-3}\end{aligned}\quad(58)$$

Where, the coefficients of the equation are

$$\begin{aligned}K_1&=\left(G_1^{\theta}+C_1^{\omega}\right)+\left(G_2^{\theta}+C_2^{\omega}\right)+G_3^{\theta}-3\\&\triangleq G_1+G_2+G_3-3\\K_2&=2\left(G_1^{\theta}+G_1^{\omega}\right)+\left(G_2^{\theta}+G_2^{\omega}\right)-3\\&\triangleq 2G_1+G_2-3\\K_3&=\left(G_1^{\theta}+G_1^{\omega}\right)-1\triangleq G_1-1\end{aligned}\quad(59)$$

For the quadratic phase input, we have

$$\varphi_k+K_1\varphi_{k-1}-K_2\varphi_{k-2}+K_3\varphi_{k-3}=0\quad(60)$$

Also

$$\varphi_{k+3}+K_1\varphi_{k+2}-K_2\varphi_{k+1}+K_3\varphi_k=0\quad(61)$$

It is easy to see that the stationary solution of (3.3.7) is

$$\varphi^*=0\quad(62)$$

3.3.1Range of Gain for Stability

The combined difference equation can be represented in the form of a set of first-order, three-dimensional state equations as

$$\begin{bmatrix}x_{k+1}\\y_{k+1}\\z_{k+1}\end{bmatrix}=\begin{bmatrix}y_k\\z_k\\-K_1z_k+K_2y_k-K_3x_k\end{bmatrix}\quad(63)$$

where $z_k=\varphi_{k+2}$, $y_k=\varphi_{k+1}$, $x_k=\varphi_k$, and $x_0=(\varphi_0, \varphi_1, \varphi_2)^T$.

The Jacobian $G'(x)=(\partial g_i/\partial x^j)$ is given by

$$G'(x)=\begin{bmatrix} 0 & 1 & 0 \\ 0 & 0 & 1 \\ -K_3 & K_2 & -K_1 \end{bmatrix} \quad (64)$$

At the fixed point $x^*=0$, we must have $|\lambda_i|<1$, i=1, 2, 3. where the λ's satisfy the characteristic equation $|\lambda I- G'(x^*)|= 0$ or

$$\lambda^3+\lambda^2(K_1)+\lambda(-K_2)+K_3=0 \quad (65)$$

By using the transformation of (3.2.10), we can get the equation in v as

$$\begin{aligned} &v^3(1+K_1-K_2+K_3)+v^2(3+K_1+K_2-3K_3) \\ &+v(3-K_1+K_2+3K_3)+(1-K_1-K_2-K_3)=0 \end{aligned} \quad (66)$$

When applying the Routh-Hurwitz criteria[12], we have

$$\begin{aligned} &1+K_1-K_2+K_3>0 \\ &3+K_1+K_2-3K_3>0 \\ &3-K_1+K_2+3K_3>0 \\ &1-K_1-K_2-K_3>0 \end{aligned} \quad (67)$$

So, we have the stable conditions for the parameters

$$\begin{aligned} &p-r>0 \\ &p+r-2>0 \\ &(p-1)G_1-p+r>0 \\ &8-(p+r+2)G_1>0 \end{aligned} \quad (68)$$

where $r=1+G_2/G_1$, $p=1+G_2/G_1+G_3/G_1$.

The conditions for faster convergence, i.e., $\rho[G'(x^*)] = 0$, can be obtained by examining (64); these are

$$K_1=K_2=K_3=0 \quad (69)$$

This means

$$G_1=G_2=G_3=1 \quad (70)$$

It is also required that $|\varphi_{k+3}|<\pi$ when $|\varphi_{k+2}|=\pi$, $|\varphi_{k+1}|=\pi$, $|\varphi_k|=\pi$ [8]. So the overall loop stable conditions independent of the initial phase tracking error can be further derived as

$$\begin{aligned} &-2<(r-p)G_1<0 \\ &4<(p+r)G_1<6 \\ &6<(p+r+2)G_1<8 \\ &0<(2+r-p)G_1<2 \end{aligned} \quad (71)$$

By comparing the analysis of this part with that of the third order PLL, it is possible to consider the combined loop as an equivalent PLL with filter coefficients $G_1^{\theta}+G_1^{\omega}$, $G_2^{\theta}+G_2^{\omega}$, G_3^{θ}, instead of G_1^{θ}, G_2^{θ} and G_3^{θ}. In this way the influence of the FLL can be inserted into the model of the PLL at a design stage. A wide bandwidth FLL allows the loop to keep stable working while the PLL is unlocked when the frequency error is within the linear range of its discriminator. At this time, the loop response is governed by the FLL and the phase error input acts like a zero-mean perturbation [18]. So from the design point, the second order FLL assisted third PLL can be optimized to a single third order PLL, this will be discussed at Section 5.

Due to the fact that the combined loop can be regarded as an equivalent third order PLL, so the convergence steps and the oscillatory behavior are almost the same as the third order PLL except that the loop parameters are different. The steps to convergences is the same as (53),

$$m<\frac{\ln\left(\dfrac{\varepsilon}{\left[(\varphi_0-\varphi_{ss})^2+(\varphi_1-\varphi_{ss})^2+(\varphi_2-\varphi_{ss})^2\right]}\right)}{\ln(L)} \quad (72)$$

The difference comes up to the value of L which is

$$L=\max\left\{\begin{aligned} &\frac{\left[-K_1\psi_2+K_2\psi_1-K_3\psi_0-\varphi_{ss}\right]^2}{\left[(\varphi_0-\varphi_{ss})^2+(\varphi_1-\varphi_{ss})^2+(\varphi_2-\varphi_{ss})^2\right]} \\ &+\frac{(\psi_1-\varphi_{ss})^2}{\left[(\varphi_0-\varphi_{ss})^2+(\varphi_1-\varphi_{ss})^2+(\varphi_2-\varphi_{ss})^2\right]} \\ &+\frac{(\psi_0-\varphi_{ss})^2}{\left[(\varphi_0-\varphi_{ss})^2+(\varphi_1-\varphi_{ss})^2+(\varphi_2-\varphi_{ss})^2\right]} \end{aligned}\right\}$$

The oscillatory behavior is the same as Section 3.3.2 except for the loop parameters.

4.Performance in the Presence of Dynamics and Noise

In this section we consider the behavior for an input with frequency ramp in the presence of noise. Due to the stochastic nature of the input phase noise, the phase tracking error is also a stochastic process. We will apply the C-K equation to study the PDF, mean and variance of the phase error. In the following, we will derive the mathematical expressions of the PDF and variance of phase error due to the input noise and present how the phase error depends on the loop parameters and input noise statistics.

4.1 The Second Order FLL

4.1.1 Steady State PDF

For the quadratic phase input, the loop equation

of the restricted (i.e. [-π, +π]) phase error process {φ(k)} is

$$\begin{aligned}&\varphi_{k+2}-2\varphi_{k+1}+\varphi_k\\&\quad=2a_2+G_1^{\omega}\left(\varphi_k+n_k^{\omega}\right)-r^{\omega}G_1^{\omega}\left(\varphi_{k+1}+n_{k+1}^{\omega}\right)\end{aligned}\tag{73}$$

Note shall be taken that the frequency noise component n^{ω} are mutually dependent for the consecutive samples due to the difference discriminator. When given (φ_k, φ_{k+1}), the pdf of (φ_{k+1},φ_{k+2}) can be achieved which is equal to that of n^{ω}. So the phase error tracking error process {φ(k)} can be regarded as a first-order, two-dimensional, discrete time, continuously variable Markov process. Therefore we may rewrite it in a set of first-order stochastic difference equations[13]. Before this, we define s(·) by

$$\varphi_k=s(k)-r^{\omega}s(k+1)+\frac{2a_2}{G_2^{\omega}}\tag{74}$$

Equation (4.1) then becomes

$$\begin{aligned}&\left[s(k+2)-2s(k+1)+s(k)\right]\\&\quad-r^{\omega}\left[s(k+3)-2s(k+2)+s(k+1)\right]\\&=G_1^{\omega}\left[s(k)-r^{\omega}s(k+1)+n_k^{\omega}\right]\\&\quad-r^{\omega}G_1^{\omega}\left[s(k+1)-r^{\omega}s(k+2)+n_{k+1}^{\omega}\right]\end{aligned}\tag{75}$$

Equation (75) may be broken up into two equivalent equations. Letting $x_1(k)=s(k)$ and $x_2(k)=s(k+1)$, one gets the following vector set of equations:

$$\begin{aligned}x_1(k+1)&=x_2(k)\\x_2(k+1)&=\left(G_1^{\omega}-1\right)x_1(k)\\&\quad+\left(2-r^{\omega}G_1^{\omega}\right)x_2(k)+G_1^{\omega}n_k^{\omega}\end{aligned}\tag{76}$$

Note that $\varphi_k=x_1(k)-r^{\omega}x_2(k)+2a_2/G_2^{\omega}$ according to(74).

The vector process {$x_1(k)$, $x_2(k)$} can be regarded as a second-order, two dimensional Markov process. Consequently, the joint PDF of $x_1(k)$, $x_2(k)$ satisfies the vector Chapman-Kolmogorov equation. The steady-state joint PDF $p(x_1,x_2)$ can be obtained by

$$\begin{aligned}&p_{k+1}\left(x_1,x_2\middle|x_{10},x_{20}\right)\\&\quad=\int_{-\infty}^{\infty}\int_{-\infty}^{\infty}q_k\left(x_1,x_2\middle|z_1,z_2\right)p_k\left(z_1,z_2\middle|x_{10},x_{20}\right)dz_1dz_2\end{aligned}\tag{77}$$

where

$x_{10}=x_1(0)$ initial value of $x_1(\cdot)$

$x_{20}=x_2(0)$ initial value of $x_2(\cdot)$

$p_k(\cdot,\cdot|\, x_{10}, x_{20})$ joint pdf of $x_1(k)$ and $x_2(k)$ given x_{10} and x_{20}

$q_k(x_1,x_2|\, z_1, z_2)$ transient joint pdf of $x_1(k+1)$, $x_2(k+1)$ and $x_3(k+1)$ given $x_1(k)=z_1$, $x_2(k)=z_2$

we can derived from (76) that

$$\begin{aligned}&q_{k+1}\left(x_1,x_2\middle|z_1,z_2\right)\\&=\delta(x_1-z_2)\times\left\{\frac{\exp(-SNR)}{2\pi G_1^{\omega}}+\frac{1}{2G_1^{\omega}}\sqrt{\frac{SNR}{\pi}}\cos\left(x^*\right)\right.\\&\quad\left.\times\exp\left[-SNR\cdot\sin^2\left(x^*\right)\right]\times\left[1+erf\left(\sqrt{SNR}\cos\left(x^*\right)\right)\right]\right\}\end{aligned}\tag{78}$$

which is independent of k and

$$x^*=\frac{1}{G_1^{\omega}}\left\{x_2-\left(2-r^{\omega}G_1^{\omega}\right)z_2-\left(G_1^{\omega}-1\right)z_1\right\}$$

When k→∞, the steady-state pdf of the phase error φ is independent of initial phase error (φ_0, φ_1) which yields[13,14]

$$p_{k+1}(x_1,x_2)=\int_{-\infty}^{\infty}q_k\left(x_2\middle|z_1,z_2\right)p_k(z_1,x_1)\,dz_1\tag{79}$$

Due to the periodicity of the discriminator, we have

$$\begin{aligned}P_k(x_1,x_2)&=\sum_{m=-\infty}^{\infty}\sum_{n=-\infty}^{\infty}p_k(x_1+2m\pi,x_2+2n\pi)\\K(x_1,x_2,z_1)&=\sum_{n=-\infty}^{\infty}q_k\left(\frac{\hat{x}+2n\pi}{G_1^{\omega}}\right)\end{aligned}\tag{80}$$

where

$$\hat{x}=x_2-\left(2-r^{\omega}G_1^{\omega}\right)x_1-\left(G_1^{\omega}-1\right)z_1+2n\pi\tag{81}$$

Consequently, the steady-state PDF $P(x_1,x_2)$ is the unique solution to the following steady-state integral equation

$$P(x_1,x_2)=\int_{-\pi}^{\pi}K(x_1,x_2,z_1)P(z_1,x_1)\,dz_1\tag{82}$$

4.1.2 Steady State Mean and Variance

The steady-state mean of the phase tracking error can be obtained by taking the expectations of both sides of (74) and (76) and letting k→∞,we have[14]

$$\begin{aligned}E[x_{1ss}]&=E[x_{2ss}]\\E[x_{2ss}]&=\left(G_1^{\omega}-1\right)E[x_{1ss}]\\&\quad+\left(2-r^{\omega}G_1^{\omega}\right)E[x_{2ss}]+G_1^{\omega}\lim_{k\to\infty}E\left[n_k^{\omega}\right]\\E[\varphi_{ss}]&=E[x_{1ss}]-r^{\omega}E[x_{2ss}]+\frac{2a_2}{G_2^{\omega}}\end{aligned}\tag{83}$$

It is easy to see that $E[n^{\omega}(k)]$ is very small compared with other terms, so we have that the steady-state mean of the phase tracking error is

$$E[\varphi_{ss}]=\frac{2a_2}{G_2^{\omega}}\tag{84}$$

Modify (73) to yield

$$\operatorname{var}(\varphi_{ss})=E\left[x_{1ss}^2\right]+r^2E\left[x_{2ss}^2\right]-2rE[x_{1ss}x_{2ss}]\tag{85}$$

By multiplying x_{1ss} with both sides of (76) and taking expectation of each term while considering the the dependency of the consecutive frequency samples, we have

$$E\left[x_{1ss}x_{2ss}\right]=\left(G_1^{\omega}-1\right)E\left[x_{1ss}^2\right]+\left(2-r^{\omega}G_1^{\omega}\right)E\left[x_{1ss}x_{2ss}\right]+\left(G_1^{\omega}\right)^2R_1^n \tag{86}$$

Squaring both sides of (76) and taking the expectation of each term, we have

$$E\left[x_{1ss}^2\right]=E\left[x_{2ss}^2\right]$$

$$E\left[x_{2ss}^2\right]=\left(G_1^{\omega}-1\right)^2E\left[x_{1ss}^2\right]+\left(2-r^{\omega}G_1^{\omega}\right)^2E\left[x_{2ss}^2\right]+\left(G_1^{\omega}\right)^2E\left[\left(n_k^{\omega}\right)^2\right]+2\left(G_1^{\omega}-1\right)\left(2-r^{\omega}G_1^{\omega}\right)E\left[x_{1ss}x_{2ss}\right]+2\left(2-r^{\omega}G_1^{\omega}\right)\left(G_1^{\omega}\right)^2R_1^n \tag{87}$$

From (85)-(87) we have

$$\mathrm{var}\left(\varphi_{ss}\right)=\frac{\left[R_1^n-R_0^n+G_1^{\omega}R_1^n\right]\left[\left(G_1^{\omega}\right)^2+2G_1^{\omega}+3\right]}{\left(3-r^{\omega}G_1^{\omega}\right)\left(G_1^{\omega}+1\right)}-\frac{2R_0^n}{\left(G_1^{\omega}+1\right)\left(G_1^{\omega}+r^{\omega}G_1^{\omega}-2\right)}-R_1^n\left(2G_1^{\omega}-r^{\omega}G_1^{\omega}+1\right) \tag{88}$$

According to [10], the correlations of n_k^{ω} are

$$R_0^n\approx\frac{2}{SNR}\left(1-e^{-0.05243\cdot SNR^2}\right)+\frac{\pi^2}{3}e^{-0.50301\cdot SNR}$$
$$R_1^n\approx-\frac{1}{2}\left(1-e^{-0.4864\cdot SNR^2}\right)R_0^n \tag{89}$$

4.2 The Third Order PLL[8]

The third order case can be concluded from [8] while just considering the quadratic phase input.

4.2.1 Steady State PDF

The third order loop difference equation can be expressed as

$$\varphi_{k+3}-3\varphi_{k+2}+3\varphi_{k+1}-\varphi_k=-p^{\theta}G_1^{\theta}\left(\varphi_{k+2}+n_{k+2}^{\theta}\right)+\left(1+r^{\theta}\right)G_1^{\theta}\left(\varphi_{k+1}+n_{k+1}^{\theta}\right)-G_1^{\theta}\left(\varphi_k+n_k^{\theta}\right) \tag{90}$$

The loop equation can be represented in the form of a set of first-order, three-dimensional state equations as

$$x_1\left(k+1\right)=x_2\left(k\right)$$
$$x_2\left(k+1\right)=x_3\left(k\right)$$
$$x_3\left(k+1\right)=\left(1-G_1^{\theta}\right)x_1\left(k\right)+\left[\left(1+r^{\theta}\right)G_1^{\theta}-3\right]x_2\left(k\right)+\left(3-p^{\theta}G_1^{\theta}\right)x_3\left(k\right)+G_1^{\theta}n^{\theta}\left(k\right) \tag{91}$$

The corresponding output equation is

$$\varphi_k=-x_1\left(k\right)+\left(1+r^{\theta}\right)x_2\left(k\right)-p^{\theta}x_3\left(k\right) \tag{92}$$

The steady-state joint pdf $p(x_1,x_2,x_3)$ can be obtained by

$$p_{k+1}\left(x_1,x_2,x_3\middle|x_{10},x_{20},x_{30}\right)=\int_{-\infty}^{\infty}\int_{-\infty}^{\infty}\int_{-\infty}^{\infty}q_k\left(x_1,x_2,x_3\middle|z_1,z_2,z_3\right)\times p_k\left(z_1,z_2,z_3\middle|x_{10},x_{20},x_{30}\right)dz_1dz_2dz_3 \tag{93}$$

where

$x_{10}=x_1(0)$ initial value of $x_1(\cdot)$
$x_{20}=x_2(0)$ initial value of $x_2(\cdot)$
$x_{30}=x_3(0)$ initial value of $x_3(\cdot)$

Using the fact that the noise $n^{\theta}(k)$ is independent of $x_1(k)$, $x_2(k)$ and $x_3(k)$, we can derived from () that

$$q_{k+1}\left(x_1,x_2,x_3\middle|z_1,z_2,z_3\right)=\delta\left(x_1-z_2\right)\delta\left(x_2-z_3\right)\times\frac{1}{G_1^{\theta}}\frac{1}{2\pi}\exp\left(-SNR\right)+\frac{1}{G_1^{\theta}}\frac{1}{2}\sqrt{\frac{SNR}{\pi}}\cos\left(x^*\right)\times\exp\left\{-SNR\cdot\sin^2\left(x^*\right)\right\}\times\left[1+erf\left(\sqrt{SNR}\cos\left(x^*\right)\right)\right] \tag{94}$$

where

$$x^*=\frac{1}{G_1^{\theta}}\left\{x_3-\left(1-G_1^{\theta}\right)z_1-\left[\left(1+r^{\theta}\right)G_1^{\theta}-3\right]z_2-\left(3-p^{\theta}G_1^{\theta}\right)z_3\right\}$$

As for $k\to\infty$, the steady-state PDF of the phase error φ exists and is unique, independent of initial phase error φ_0. Therefore, $\lim_{k\to\infty}p_k(\varphi|\varphi_0)\triangleq p(\varphi)$ could be obtained by

$$p_{k+1}\left(x_1,x_2,x_3\right)=\int_{-\infty}^{\infty}q_k\left(x_3\middle|z_1,z_2,z_3\right)p_k\left(z_1,x_1,x_2\right)dz_1 \tag{95}$$

We introduce periodicity into the pdf of the phase tracking error as

$$P_k\left(x_1,x_2,x_3\right)=\sum_{m=-\infty}^{\infty}\sum_{n=-\infty}^{\infty}\sum_{l=-\infty}^{\infty}p_k\left(x_1+2m\pi,x_2+2n\pi,x_3+2l\pi\right) \tag{96}$$

As for the conditional PDF of the phase tracking error, by using periodicity we have

$$K\left(x_1, x_2, x_3, z_1\right) = \sum_{n=-\infty}^{\infty} q_k\left(\frac{\hat{x} + 2n\pi}{G_1^{\theta}}\right) \tag{97}$$

where the argument ẋ is

$$\begin{aligned}\hat{x} = x_3 - \left(3 - p^{\theta} G_1^{\theta}\right) x_2 - \left[\left(1 + r^{\theta}\right) G_1^{\theta} - 3\right] x_1 \\ - \left(1 - G_1^{\theta}\right) z_1 + 2n\pi\end{aligned} \tag{98}$$

Consequently, (95) becomes

$$\begin{aligned}&P_{k+1}\left(x_1, x_2, x_3\right) \\ &\quad = \int_{-\pi}^{\pi} K\left(x_1, x_2, x_3, z_1\right) P_k\left(z_1, x_1, x_2\right) dz_1\end{aligned} \tag{99}$$

As for k→∞, the steady-state PDF is independent of the subscript k, which yields

$$P\left(x_1, x_2, x_3\right) = \int_{-\pi}^{\pi} K\left(x_1, x_2, x_3, z_1\right) P\left(z_1, x_1, x_2\right) dz_1 \tag{100}$$

4.2.2 Steady State Mean and Variance

By taking the expectations of (91) the steady-state mean of the phase error is obtained as

$$E\left[\varphi_{ss}\right] = 0 \tag{101}$$

the steady-state variance of the phase error is [6]

$$\begin{aligned}\operatorname{var}\left[\varphi_{ss}\right] &= E\left[\varphi_{ss}^2\right] - \left\{E\left[\varphi_{ss}\right]\right\}^2 \\ &= \frac{\left[\left(r^2 + 4p^2 - 8rp\right) + \left(2p + p^2 + 2rp + rp^2 - 2r - 3r^2 - r^3\right)\right] G_1 E\left[n_{\theta}^2\right]}{16\left(r - p\right) + \left(-12r + 12p - 10r^2 + 2p^2 + 8rp\right) G_1 + \left(1 + r\right)\left(2r + r^2 - 2p - p^2\right) G_1^2}\end{aligned} \tag{102}$$

4.3 The Combined Tracking Loop

4.3.1Steady-State PDF of Phase Error

The phase tracking error in the presence of noise can be represented on z-plane as

$$\Phi\left(z\right) = \frac{\Theta\left(z\right) - n_k^{\omega} D\left(z\right) F^{\omega}\left(z\right) N\left(z\right) - n_k^{\theta} F^{\theta}\left(z\right) N\left(z\right)}{1 + \left[K^{\theta} F^{\theta}\left(z\right) + D\left(z\right) K^{\omega} F^{\omega}\left(z\right)\right] N\left(z\right)} \tag{103}$$

For the quadratic input phase, the loop difference equation of the restricted phase error process {φ(k)} is, from (103) which can be presented as

$$\begin{aligned}&\varphi_{k+3} - 3\varphi_{k+2} + 3\varphi_{k+1} - \varphi_k \\ &\quad = -p^{\theta} G_1^{\theta}\left(\varphi_{k+2} + n_{k+2}^{\theta}\right) + \left(1 + r^{\theta}\right) G_1^{\theta}\left(\varphi_{k+1} + n_{k+1}^{\theta}\right) \\ &\qquad - G_1^{\theta}\left(\varphi_k + n_k^{\theta}\right) - r^{\omega} G_1^{\omega}\left(\varphi_{k+2} + n_{k+2}^{\omega}\right) \\ &\qquad + \left(1 + r^{\omega}\right) G_1^{\omega}\left(\varphi_{k+1} + n_{k+1}^{\omega}\right) - G_1^{\omega}\left(\varphi_k + n_k^{\omega}\right)\end{aligned} \tag{104}$$

In order to use the results of the third order PLL, we must do some modification on equation (104) as

$$\begin{aligned}G &= G_1^{\theta} + G_1^{\omega} \\ P &= \frac{p^{\theta} G_1^{\theta} + r^{\omega} G_1^{\omega}}{G_1^{\theta} + G_1^{\omega}} \\ R &= \frac{\left(1 + r^{\theta}\right) G_1^{\theta} + \left(1 + r^{\omega}\right) G_1^{\omega}}{G_1^{\theta} + G_1^{\omega}} \\ N_{k+2} &= \frac{G\left(p^{\theta} G_1^{\theta} n_{k+2}^{\theta} + r^{\omega} G_1^{\omega} n_{k+2}^{\omega}\right)}{p^{\theta} G_1^{\theta} + r^{\omega} G_1^{\omega}} \\ N_{k+1} &= \frac{G\left[\left(1 + r^{\theta}\right) G_1^{\theta} n_{k+1}^{\theta} + \left(1 + r^{\omega}\right) G_1^{\omega} n_{k+1}^{\omega}\right]}{\left(1 + r^{\theta}\right) G_1^{\theta} + \left(1 + r^{\omega}\right) G_1^{\omega}} \\ N_k &= \frac{G\left(G_1^{\theta} n_k^{\theta} + G_1^{\omega} n_k^{\omega}\right)}{G_1^{\theta} + G_1^{\omega}}\end{aligned} \tag{105}$$

By substituting (105) into (104) yields

$$\begin{aligned}&\varphi_{k+3} - 3\varphi_{k+2} + 3\varphi_{k+1} - \varphi_k \\ &\quad = -PG\left(\varphi_{k+2} + N_{k+2}\right) \\ &\qquad + RG\left(\varphi_{k+1} + N_{k+1}\right) - G\left(\varphi_k + N_k\right)\end{aligned} \tag{106}$$

Now the form of (106) is the same as that of (91)except of the loop parameters and noise character. So it can be represented in the form of a set of first-order, three-dimensional state equations as

$$\begin{aligned} x_1(k+1) &= x_2(k) \\ x_2(k+1) &= x_3(k) \\ x_3(k+1) &= (3-PG)x_3(k) + (RG-3)x_2(k) \\ &\quad + (1-G)x_1(k) + GN_k \end{aligned} \tag{107}$$

The corresponding output equation is

$$\varphi_k = -x_1(k) + Rx_2(k) - Px_3(k) \tag{108}$$

Comparing (107) and (108) with (91) and (92), we know that the equation form are the same. So, all the methods studying the steady-state character of the third-order PLL can be used to analyze that of the combined loop. Thus, steady-state PDF suits to the following equation

$$P(x_1, x_2, x_3) = \int_{-\pi}^{\pi} K(x_1, x_2, x_3, z_1) P(z_1, x_1, x_2)\, dz_1 \tag{109}$$

The expressions for K and P are

$$\begin{aligned} &P_k(x_1, x_2, x_3) \\ &= \sum_{m=-\infty}^{\infty} \sum_{n=-\infty}^{\infty} \sum_{l=-\infty}^{\infty} p_k(x_1 + 2m\pi, x_2 + 2n\pi, x_3 + 2l\pi) \end{aligned} \tag{110}$$

$$K(x_1, x_2, x_3, z_1) = \sum_{n=-\infty}^{\infty} q_k\left(\frac{\hat{x} + 2n\pi}{G}\right) \tag{111}$$

where the argument and transient PDF are

$$\begin{aligned} \hat{x} &= x_3 - (3-PG)x_2 - (RG-3)x_1 \\ &\quad - (1-G)z_1 + 2n\pi \end{aligned} \tag{112}$$

$$\begin{aligned} &q_k(x_1, x_2, x_3 | z_1, z_2, z_3) \\ &= \delta(x_1 - z_2)\delta(x_2 - z_3) \\ &\times \frac{1}{G}\frac{1}{2\pi}\exp(-SNR) + \frac{1}{G}\frac{1}{2}\sqrt{\frac{SNR}{\pi}}\cos(x^*) \\ &\times \exp\left\{-SNR \cdot \sin^2(x^*)\right\} \\ &\times \left[1 + erf\left(\sqrt{SNR}\cos(x^*)\right)\right] \end{aligned} \tag{113}$$

and

$$x^* = \frac{1}{G}\left[x_3 - (1-G)z_1 - (RG-3)z_2 - (3-PG)z_3\right]$$

The illustrations for symbols P, K, q and z_1, z_2, z_3 are the same as the explanations for equation (93).

4.3.2 Steady-State Mean and Variance

By taking the expectations of (91) the steady-state mean of the phase error is obtained as

$$E[\varphi_{ss}] = 0 \tag{114}$$

the steady-state variance of the phase error is

$$\begin{aligned} \mathrm{var}[\varphi_{ss}] &= E\left[\varphi_{ss}^2\right] - \{E[\varphi_{ss}]\}^2 \\ &= \left(1 + R^2 + P^2\right)E\left[x_{1ss}^2\right] - 2R(P+1)E[x_{2ss}x_{3ss}] \end{aligned} \tag{115}$$

Multiply $x_2(k)$ with both sides of (4107) and taking expectation of each term while considering the the dependency of the consecutive two samples, we have

$$\begin{aligned} E[x_{2ss}x_{3ss}] &= (RG-3)E\left[x_{2ss}^2\right] \\ &\quad + (4 - PG - G)E[x_{2ss}x_{3ss}] + G^2R_1^N \end{aligned} \tag{116}$$

Squaring both sides of (107) and taking the expectation of each term, we have

$$\begin{aligned} E\left[x_{3ss}^2\right] &= \left[(3-PG)^2 + (RG-3)^2 + (1-G)^2\right]E\left[x_{3ss}^2\right] \\ &\quad + \left[2(RG-3)(4-PG-G)\right]E[x_{2ss}x_{3ss}] \\ &\quad + 2G^2(3-PG)R_1^N + G^2R_0^N \end{aligned} \tag{117}$$

In equation (117), we have supposed that $E[x_{1ss}x_{2ss}]=E[x_{2ss}x_{3ss}]$ for simplicity. According to the analysis of section 2, n^{θ} and n^{ω} have the same PDF, so the correlations of N_k are

$$\begin{aligned} R_1^N &= \frac{G^2\left(G_1^{\omega}\right)^2 R_1^{\omega}}{\left(G_1^{\theta} + G_1^{\omega}\right)^2} \\ R_0^N &= \frac{G^2\left[\left(G_1^{\theta}\right)^2 R_0^{\theta} + \left(G_1^{\omega}\right)^2 R_0^{\omega}\right]}{\left(G_1^{\theta} + G_1^{\omega}\right)^2} \end{aligned} \tag{118}$$

Where R_0^N, R_1^N are the correlations of noise N_k with correlate spaces are zero and one respectively. R_0^{ω}, R_1^{ω} are the correlations of n^{ω}; R_0^{θ}, R_1^{θ} are the correlations of n^{θ}.

From equations (116), (117) and (118), we have the variance of the combined loop as

$$\begin{aligned} \mathrm{var}[\varphi_{ss}] = &\frac{\left[-G^2\left(G + 6R + 6PR + GP^2 + GP^3 - GR^2 - 3P^2 - 3R^2 + GP - GPR^2 - 3\right)\right]R_0^N + G^2R_1^N\left[2G^2P^4 + 2G^2P^3\right.}{} \\ &\left. - 2G^2P^2R^2 + 2G^2P^2 - 2G^2PR^2 + 2G^2P - 18GP^3 + 16GP^2R - 12GP^2 + 6GPR^2 + 28GPR - 18GP - 8GR^3\right. \\ &\left. + 12GR^2 - 4GR - 12G + 42P^2 - 72PR + 42R^2 - 72R + 42\right] \\ &\frac{}{G^3\left(P^3 + P^2 - PR^2 + P - R^2 + 1\right) + G^2\left(-9P^2 + 6PR - 8P + 5R^2 + 6R - 5\right) + G(18P - 30R + 6) + 18} \end{aligned} \tag{119}$$

5 Loop Optimization

This section will discuss the optimization for the FLL assisted PLL at a design stage. The aim is to find the optimal loop filter structure. The method to design the digital loop filters is based on an optimization process that poses the tradeoff between noise bandwidth and dynamics in a quadratic function which is minimized for a particular dynamic input.

5.1 Optimum Filter for Arbitrary Input

Assuming the performance function to be[15, 16]

$$Q = E\left[n_0^2(k)\right] + \lambda \sum_k e^2(k) \tag{120}$$

Where $e(k) = \theta(k) - \hat{\theta}(k)$ is the deterministic component of the phase difference between incoming and generated phase. The parameter λ is determined on the basis of noise bandwidth considerations. The noise part of (120) can be expressed in terms of the closed loop transfer function H(z) as

$$E\left[n_0^2(k)\right] = \frac{1}{2\pi j}\oint_{|z|=1} \Phi_{n_0 n_0}(z)\frac{dz}{z} \tag{121}$$

Where Φ_{n0n0} is the noise spectral density of noise n_0 and is related to the input noise spectral density as

$$\Phi_{n_0 n_0}(z) = H(z)H\left(z^{-1}\right)\Phi_{n_i n_i}(z) \tag{122}$$

And the closed loop transfer function is

$$H(z) = \frac{F(z)N(z)}{1 + F(z)N(z)} \tag{123}$$

According to Parseval equation, the second part of the performance function can be rewritten as

$$\sum_k e^2(k) = \frac{1}{2\pi j}\oint_{|z|=1}\left[1 - H(z)\right]\left[1 - H\left(z^{-1}\right)\right]\Phi_{\theta\theta}(z)\frac{dz}{z} \tag{124}$$

Where Θ(z) is the z transformation of θ(k) and $\Theta_{\theta\theta}(z) = \Theta(z)\,\Theta(z^{-1})$.

From (121) and (124), equation (120) can be expressed as

$$Q = \frac{1}{2\pi j}\oint_{|z|=1}\left[\lambda\Phi_{\theta\theta}(z) + P(z)W(z)W\left(z^{-1}\right) - \lambda W(z)N(z)\Phi_{\theta\theta}(z) - \lambda W\left(z^{-1}\right)N\left(z^{-1}\right)\Phi_{\theta\theta}(z)\right]\frac{dz}{z} \tag{125}$$

Where

$$H(z) = W(z)N(z) \tag{126}$$

And

$$P(z) = \left[\Phi_{n_i n_i}(z) + \lambda\Phi_{\theta\theta}(z)\right]N(z)N\left(z^{-1}\right) \tag{127}$$

Let $W(z) = W_0(z) + \varepsilon\eta(z)$, where $W_0(z)$ is the optimal loop transfer function and εη(z) is the variation to be minimized on the true optimum $W_0(z)$. Substitute this equation into (125) and setting the variation of Q to zero at ε equals zero completes the standard vibrational procedure[16].

$$\left.\frac{\partial Q\left[W_0(z) + \varepsilon\eta(z)\right]}{\partial\varepsilon}\right|_{\varepsilon=0} = \frac{1}{2\pi j}\oint_{|z|=1}\left[P(z)W(z)\eta\left(z^{-1}\right) + P(z)W\left(z^{-1}\right)\eta(z) - \lambda\eta(z)N(z)\Phi_{\theta\theta}(z) - \lambda\eta\left(z^{-1}\right)N\left(z^{-1}\right)\Phi_{\theta\theta}(z)\right]\frac{dz}{z} \tag{128}$$

In order to keep all the terms in (128) split into factors having poles in either, but not both, the inside or outside the unit circle, it is convenient to define

$$P(z) = P^+(z)P^-(z) \tag{129}$$

Where all the poles in $P^+(z)$ are inside the unit circle and $P^-(z)$ has all the poles outside the unit circle. So, we have from (128) that

$$\left.\frac{\partial Q\left[W_0(z) + \varepsilon\eta(z)\right]}{\partial\varepsilon}\right|_{\varepsilon=0} = \frac{1}{2\pi j}\oint_{|z|=1}\left\{\eta\left(z^{-1}\right)P^-(z)\left[P^+(z)W_0(z) - \lambda\frac{N\left(z^{-1}\right)\Phi_{\theta\theta}(z)}{P^-(z)}\right] \eta(z)P^+(z)\left[P^-(z)W_0\left(z^{-1}\right) - \lambda\frac{N(z)\Phi_{\theta\theta}(z)}{P^+(z)}\right]\right\}\frac{dz}{z} \tag{130}$$

From (130), we can find that the poles in the first part are z_i and those in the second part are z_i^{-1}, and we have[17]

$$\oint f\left(z^{-1}\right)\frac{dz}{z} = \oint f(z)\frac{dz}{z}$$

So, (130) can be reduced to be

$$\left.\frac{\partial Q\left[W_0(z) + \varepsilon\eta(z)\right]}{\partial\varepsilon}\right|_{\varepsilon=0} = \frac{1}{\pi j}\oint_{|z|=1}\left\{\eta\left(z^{-1}\right)P^-(z)\left[z^{-1}P^+(z)W_0(z) - \lambda\frac{N\left(z^{-1}\right)\Phi_{\theta\theta}(z)}{zP^-(z)}\right]\right\} \tag{131}$$

Taking (131) equal to zero yields

$$W_0(z)=\frac{z\cdot\left[\dfrac{\lambda N(z^{-1})\Phi_{\theta\theta}(z)}{z\cdot P^{-}(z)}\right]_{+}}{P^{+}(z)} \tag{132}$$

Where $[\ ]_+$ illustrates that all the poles are outside the unit circle. The corresponding optimal loop filters are

$$F(z)=\frac{W_0(z)}{1-W_0(z)N(z)} \tag{133}$$

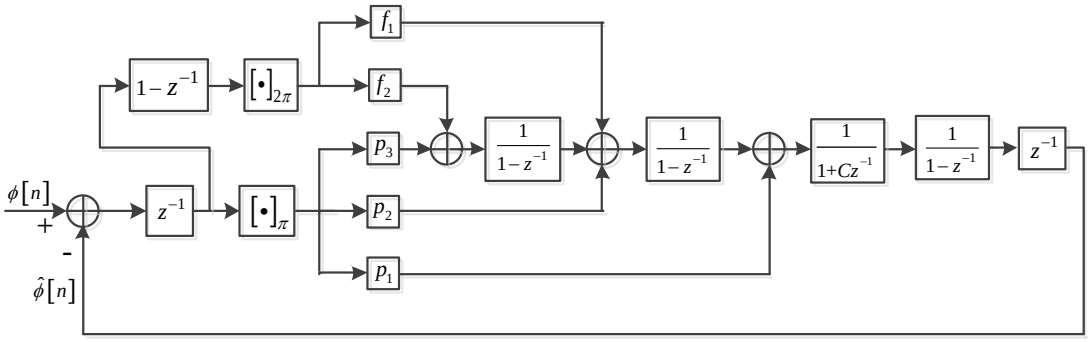

Fig. 12. The structure of the optimum PLL for tracking Doppler rates

5.2Optimal Filter for Doppler Rates

Utilizing the analysis method of Section 5.1, the optimum filter for a Doppler rate signal can be derived. According to [17,18], the optimal filter for a frequency ramp signal can be expressed as

$$F(z)=\frac{A-Bz^{-1}+cz^{-2}}{(1-z^{-1})^3(1+cz^{-1})} \tag{134}$$

For the purpose of implementation, it is desirable to use a cascade of accumulators. Then (134) can be rewritten as

$$F(z)=\frac{p_3+(f_2+p_2)(1-z^{-1})+(f_1+p_1)(1-z^{-1})^2}{(1-z^{-1})^3(1+p_1z^{-1})} \tag{135}$$

Where $f_1+p_1=C$, $f_2+p_2=B-2C$ and $p_3=A-B+C$. The corresponding structure of the optimum loop is illustrated in Figure 12.And A, B and C satisfy the following equations

$$A=6-3z_s+z_d,\ B=8-3z_s+z_p,\ C=3-z_s$$
$$z_s=z_1+z_2+z_3,\ z_p=z_1z_2z_3,\ z_d=z_1z_2+z_1z_3+z_2z_3 \tag{136}$$

Where z_1, z_2 and z_3 are the solutions of the following equations

$$z_{1,2}+z_{1,2}^{-1}=2-\frac{1\pm j\sqrt{3}}{2}\sqrt[3]{\nu}$$
$$z_3+z_3^{-1}=2+\sqrt[3]{\nu} \tag{137}$$
$$\nu=\dot{\Delta}\omega^2T^4\gamma^2$$

And the corresponding frequency ramp is

$$\Phi(z)=\frac{\dot{\Delta}\omega T^2}{(1-z^{-1})^3} \tag{138}$$

The relationship of loop noise equivalent bandwidth versus loop parameter ν is shown in Figure 13. When designing a loop, we shall first choose the appropriate noise bandwidth so as to get the ν value and substitute it into (137), z_1, z_2 and z_3 will be calculated, then A, B and C will be derived by using equation (136). Thus, we get f_1 and f_2, p_1, p_2 and p_3.

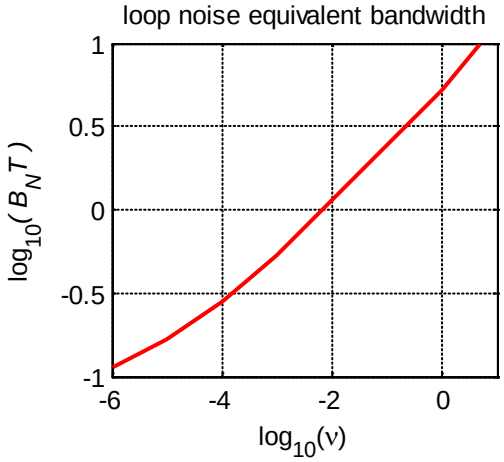

Fig. 13. Loop noise equivalent bandwidth

5.3 Design Example: Loops for Responders

Taking the trajectory in Section 1 into account, we model the input dynamic as an acceleration step, which becomes quadratic ramp in terms of phase and a linear one in term of frequency. For these inputs, the optimal loop filter was obtained in Section 5.2.

A typical rule of thumb for keeping a reasonable distance from the pull-out values of the

loop is that the peak of the error transient has a maximum value given by half the linear range of the phase discriminator, an eight of cycle [17]. Always we takeB_NT<1 to keep loop stable. So, we have B_NT=0.125(i.e. -0.9 for log(·)) which means $\nu=3\times10^{-4}$. Substitute this values into (137), (136) and (135) yields A=0.6173, B=1.105 and C=0.5.

5.4Stable Range for the Optimum Loop

The optimal loop has an extra pole at z= – C compared with the traditional one. So, the loop transfer function is

$$\begin{aligned}\Theta(z)\left[1+(C-3)z^{-1}+3(1-C)z^{-2}+(3C-1)z^{-3}-Cz^{-4}\right]\\ =\Phi\left[1+(C-3)z^{-1}+(p_1+p_2+p_3-3C+3)z^{-2}\right.\\ \left.+(3C-2p_1-p_2-1)z^{-3}+(p_1-C)z^{-4}\right.\end{aligned} \tag{139}$$

So, we have corresponding difference equation as

$$\begin{aligned}\theta_{k+4}+(C-3)\theta_{k+3}+3(1-C)\theta_{k+2}+(3C-1)\theta_{k+1}-C\theta_k\\ =\varphi_{k+4}+(C-3)\varphi_{k+3}+(p_1+p_2+p_3-3C+3)\varphi_{k+2}\\ +(3C-2p_1-p_2-1)\varphi_{k+1}+(p_1-C)\varphi_k\end{aligned} \tag{140}$$

As for the quadratic phase input like (26), we have

$$\begin{aligned}\varphi_{k+4}=(3-C)\varphi_{k+3}-(p_1+p_2+p_3-3C+3)\varphi_{k+2}\\ +(2p_1+p_2+1-3C)\varphi_{k+1}+(C-p_1)\varphi_k\end{aligned} \tag{141}$$

It's easy to see that the fixed point is

$$\varphi^*=0 \tag{142}$$

This equation can be rewritten in a set of first-order difference equations as

$$\begin{bmatrix}w_{k+1}\\x_{k+1}\\y_{k+1}\\z_{k+1}\end{bmatrix}=\begin{bmatrix}x_k\\y_k\\z_k\\\kappa_1z_k-\kappa_2y_k+\kappa_3x_k+\kappa_4w_k\end{bmatrix} \tag{143}$$

where $w_k=\varphi_k$, $w_0=(\varphi_0,\ \varphi_1,\ \varphi_2,\ \varphi_3)^T$ and the loop parameters are

$$\begin{aligned}\kappa_1&=3-C\\ \kappa_2&=p_1+p_2+p_3-3C+3\\ &\triangleq pp_1-3C+3\\ \kappa_3&=2p_1+p_2+1-3C\\ &\triangleq(1+r)p_1+1-3C\\ \kappa_4&=C-p_1\end{aligned} \tag{144}$$

where$r = 1 + p_2/p_1$, $p = r + p_3/p_1$.

The Jacobian $G'(x)=(\partial g_i/\partial x^j)$ is given by

$$G'(x)=\begin{bmatrix}0&1&0&0\\0&0&1&0\\0&0&0&1\\\kappa_4&\kappa_3&-\kappa_2&\kappa_1\end{bmatrix} \tag{145}$$

At the fixed point $x^* = 0$, we must have $|\lambda_i|<1$, i=1, 2, 3. where the λ's satisfy the characteristic equation $|\lambda I- G'(x^*)|= 0$ or

$$\lambda^4+\lambda^3(-\kappa_1)+\lambda^2(\kappa_2)+\lambda(-\kappa_3)+(-\kappa_4)=0 \tag{146}$$

By utilizing (48) in (146), we have

$$\begin{aligned}\nu^4\left[\kappa_2-\kappa_1-\kappa_3-\kappa_4+1\right]+\nu^3\left[2\kappa_3-2\kappa_1+4\kappa_4+4\right]\\ +\nu^2\left[6-6\kappa_4-2\kappa_2\right]+\nu\left[2\kappa_1-2\kappa_3+4\kappa_4+4\right]\\ +\left[\kappa_1+\kappa_2+\kappa_3-\kappa_4+1\right]=0\end{aligned} \tag{147}$$

When the Routh-Hurwitz criteria is applied, we have

$$\begin{aligned}&\kappa_2-\kappa_1-\kappa_3-\kappa_4+1>0\\ &2\kappa_3-2\kappa_1+4\kappa_4+4>0\\ &6-6\kappa_4-2\kappa_2>0\\ &2\kappa_1-2\kappa_3+4\kappa_4+4>0\\ &\kappa_1+\kappa_2+\kappa_3-\kappa_4+1>0\end{aligned} \tag{148}$$

Also we have from (144) and (148) that

$$\begin{aligned}&p-r>0\\ &r-1>0\\ &p<3\\ &4C-(r+3)p_1+4>0\\ &-8C+(p+r+2)p_1+8>0\end{aligned} \tag{149}$$

From (149), we can derive the region for C as

$$\begin{aligned}&-1<C<1, \qquad \textit{for } r \textit{ and } p\\ &\frac{(r+3)p_1-4}{4}<C<\frac{(p+r+2)p_1+8}{8}, \qquad \textit{given } r \textit{ and } p\end{aligned} \tag{150}$$

6 Conclusion

The performance of a second order FLL assisted third order PLL for the spread spectrum responder carrier phase tracking has been investigated. Stable regions, oscillatory behavior and steps for convergence for the FLL, PLL and the combined loop have been derived by taking them as a fixed point problem in the absence of noise.The mean and variance of these three loops have been studied in the presence of noise. At last, we have discussed the optimizations for the assisted tracking loop. This work provides an important reference in the design

for high dynamic carrier tracking in digital domain.

Acknowlegement

This work was supported by National High Technology Research and Development Program of China (2011AA7014053).

References:

[1] Shen Rongjun, Zhao Jun. Development Tendency and Strategy of Space TT&C Technology of Our Country. *Journal of Astronautics*, 3(22), 2001.

[2] GUO Qi, GAO Fei and LI Guo-min. Analysis for performance and measures of anti -interference in a Spectrum TT&C System. *Journal of Spacecraft TT&C Technology*, 2005, 24(1): 1591-1595.

[3] HAO Xue-kun, MA Wen-feng, FANG Hua and etc. The Study of Simulation for Tracking Statellite Doppler Shift Using Third-order Phase-locked loop. *Journal of System Simulation*, 2004, 4(16): 625-627.

[4] Vilnrotter, V.A.; Hinedi, S.; Kumar, R., "Frequency estimation techniques for high dynamic trajectories," *Aerospace and Electronic Systems, IEEE Transactions on* , vol.25, no.4, pp.559,577, Jul 1989.

[5] Ward, Phillip W., "Performance Comparisons Between FLL, PLL and a Novel FLL-Assisted-PLL Carrier Tracking Loop Under RF Interference Conditions," *Proceedings of the 11th International Technical Meeting of the Satellite Division of The Institute of Navigation (ION GPS 1998)*, Nashville, TN, September 1998, pp. 783-795.

[6] Curran, J.T.; Lachapelle, G.; Murphy, C.C., "Improving the Design of Frequency Lock Loops for GNSS Receivers," *Aerospace and Electronic Systems, IEEE Transactions on* , vol.48, no.1, pp.850,868, Jan. 2012.

[7] Kaplan E D. *Understanding GPS:Principles and Applications*, Artech House, Chapter 5, pp.153-241.

[8] Weihua Zhuang, "Performance analysis of GPS carrier phase observable," *IEEE Transactions on Aerospace and Electronic Systems*, vol.32, no.2, pp.754,767, April 1996.

[9] Yu, W., Lachapelle, G., Skone, S., "PLL Performance for Signals in the Presence of Thermal Noise, Phase Noise, and Ionospheric Scintillation," *Proceedings of the 19th International Technical Meeting of the Satellite Division of The Institute of Navigation (ION GNSS 2006)*, Fort Worth, TX, September 2006, pp. 1341-1357.

[10] P. Crosta, A Novel Approach to the Performance Evaluation of an Arctangent Discriminator for Phase Locked Loop and application to the carrier tracking of the Ionospheric Scintillation, (ENC-GNSS), Naples, Italy, May 2009.

[11] Osborne, H., "Stability Analysis of an Nth Power Digital Phase-Locked Loop--Part I: First-Order DPLL," *Communications, IEEE Transactions on* , vol.28, no.8, pp.1343,1354, Aug 1980.

[12] Osborne, H., "Stability Analysis of an Nth Power Digital Phase-Locked Loop--Part II: Second- and Third-Order DPLL's," *Communications, IEEE Transactions on* , vol.28, no.8, pp.1355,1364, Aug 1980.

[13] Weinberg, Aaron; Bede Liu, "Discrete Time Analyses of Nonuniform Sampling First- and Second-Order Digital Phase Lock Loops," *Communications, IEEE Transactions on* , vol.22, no.2, pp.123,137, Feb 1974.

[14] Jae Lee; Chong Un, "Performance Analysis of Digital Tanlock Loop," *Communications, IEEE Transactions on* , vol.30, no.10, pp.2398,2411, Oct 1982.

[15] Kazemi, Pejman L., "Optimum Digital Filters for GNSS Tracking Loops," *Proceedings of the 21st International Technical Meeting of the Satellite Division of The Institute of Navigation* (ION GNSS 2008), Savannah, GA, September 2008, pp. 2304-2313.

[16] Jaffe, R.; Rechtin, E., "Design and performance of phase-lock circuits capable of near-optimum performance over a wide range of input signal and noise levels," *Information Theory, IRE Transactions on* , vol.1, no.1, pp.66,76, March 1955.

[17] Pedro A. Roncagliolo, Javier G. García, and Carlos H. Muravchik, “Optimized Carrier Tracking Loop Design for Real-Time High-Dynamics GNSS Receivers,” *International Journal of Navigation and Observation*, vol. 2012, Article ID 651039, 18 pages, 2012.

[18] P. A. Roncagliolo, C. E. De Blasis and C.H. Muravchik, “GPS Digital Tracking Loops Design for High Dynamic Launching Vehicles,” *in Proceedings of The 9th International Symposium on Spread Spectrum Techniques and Applications*, ISSSTA 2006, Manaos, Brazil, August, 2006.